Proceedings of the 28th IEEE
EMBS Annual International Conference
New York City, USA, Aug 30-Sept 3, 2006

Maintenance of Ventricular Fibrillation in Heterogeneous Ventricle

Hermenegild J. Arevalo and Natalia A. Trayanova

Abstract—**Although ventricular fibrillation (VF) is the prevalent cause of sudden cardiac death, the mechanisms that underlie VF remain elusive. One possible explanation is that VF is driven by a single robust rotor that is the source of wavefronts that break-up due to functional heterogeneities. Previous 2D computer simulations have proposed that a heterogeneity in background potassium current (IK1) can serve as the substrate for the formation of mother rotor activity. This study incorporates IK1 heterogeneity between the left and right ventricle in a realistic 3D rabbit ventricle model to examine its effects on the organization of VF. Computer simulations show that the IK1 heterogeneity contributes to the initiation and maintenance of VF by providing regions of different refractoriness which serves as sites of wave break and rotor formation. A single rotor that drives the fibrillatory activity in the ventricle is not found in this study. Instead, multiple sites of reentry are recorded throughout the ventricle. Calculation of dominant frequencies for each myocardial node yields no significant difference between the dominant frequency of the LV and the RV. The 3D computer simulations suggest that IK1 spatial heterogeneity alone can not lead to the formation of a stable rotor.**

I. Introduction

HEART disease is a prevalent cause of mortality in the United States. In most cases, sudden cardiac death is preceded by ventricular fibrillation (VF), an episode where the heart experiences asynchronous electrical rhythm defined by rapid and erratic conduction patterns. Currently, the mechanisms that underlie VF are not well understood. Most insights into fibrillation are based from experimental studies that are limited to characterizing the surface activities [1]. In light of this limitation, several theories have been proposed about the organization of cardiac electrical activity during VF.

One is the multiple wavelet theory which posits that the complex activation pattern that defines VF is driven by spontaneous wave breakup throughout the ventricle [2][3]. Another theory is based on studies that have discovered the formation of a single rotor that drives the fibrillatory activity [4] [5]. Samie et al. have found such mother rotor activity during VF in guinea pigs. Spectral analysis of guinea pig hearts yielded the presence of regions of dominant frequencies (DF) scattered throughout the heart. The highest DF domains were located in the left ventricle (LV). Fluorescence imaging of the epicardium showed the presence of persistent rotor activity in the regions of high frequency. Single cell electrophysiological studies resulted in the discovery of a higher outward component of the background IK1 current in the LV compared to the RV. Postulating that the difference in IK1 current is the substrate for the mother rotor activity, computer simulations were performed using a 2D monodomain tissue that incorporated the IK1 heterogeneity. The simulations support the proposed mechanism observed in the experimental study.

The goal of this study is to incorporate IK1 heterogeneity into our accurate rabbit ventricular model and determine whether IK1 heterogeneity, by itself, can lead to the formation of regions of dominant frequency and a persistent rotor that drives VF.

Manuscript received April 3, 2006.

H. J. Arevalo and N. A. Trayanova are with the Biomedical Engineering Department of Tulane University, New Orleans, LA 70118 USA (phone: 504-314-2929; fax: 504-862-8779; e-mail: hareval@tulane.edu, nataliat@tulane.edu).

II. Methods

A. 2D simulation

The 2D study was performed on a 4 cm x 4 cm bidomain sheet. The bidomain model defines the intracellular space, extracellular space, and the cell membrane continuously over the entire space. The bidomain equations are:

$$\nabla \cdot (\hat{\sigma}_i \nabla \Phi_i) = I_m \quad (1)$$

$$\nabla \cdot (\hat{\sigma}_e \nabla \Phi_e) = -(I_m + I_{stim}) \quad (2)$$

where I_{stim} is transmembrane current density stimulus, σ_i and σ_e are the intracellular and extracellular conductivity tensors, Φ_i and Φ_e are the intracellular and extracellular potentials, I_m is the transmembrane volume current density, which is composed of the ionic current, I_{ion}, and capacitive current, $C_m \delta V_m / \delta t$. A modified version of the Luo-Rudy model is used to define I_{ion} [6]. The modification involves incorporating spline functions that model the dynamics of the IK1 channel. Two different IK1 currents are used, one for LV and the other for RV, based on patch clamp studies performed by [5]. Due to the IK1 current difference, the LV exhibits shorter action potential duration (APD) and lower resting potential than the RV [Fig. 1A].

The 2D model incorporated heterogeneity by including a 2 cm x 2 cm square region in the center of the tissue that is modeled as LV and the surrounding tissue is modeled as RV. A spiral wave is initiated in the LV region by an S1-S2 stimulation protocol. A planar wave is delivered to the left edge of the tissue followed by a premature stimulus delivered over the lower left quadrant of the tissue at the refractory tail of the planar wave.

1-4244-0033-3/06/$20.00 ©2006 IEEE.

B. 3D simulation

For the 3D study, we used the anatomically accurate finite-element bidomain rabbit ventricular model described in [7]. Our rabbit model features accurate geometry and realistic fiber architecture and includes a surrounding bath and blood in the cavities. The fiber architecture and unequal anisotropy are accounted for in the bidomain equations via the conductivity tensors. Numerical aspects regarding the finite-element solver can be found in [8]. The LV/RV demarcation is set between the LV and the septum with the septum being modeled as part of the RV [Fig 1c].

Prior to the induction of VF, the model was paced for 5 beats from the apex at a coupling interval of 250 ms to stabilize the action potential duration (APD). VF was induced via fast pacing on the LV epicardium at a rate of 20 Hz for 400 ms. Seven seconds of VF were simulated. The combination of the bidomain formulation, expansive 3D geometry, accurate ionic model, and a long episode of VF resulted in computational times that were in the order of several weeks. Other VF initiation sites were also investigated but not presented in this study.

Fast Fourier transform (FFT) was performed for the transmembrane potential trace of all 63,886 nodes defined in the myocardium. The power spectrum is calculated and the peak is taken to be the dominant frequency of each trace. A DF map is constructed to observe the distribution of DF and the presence of DF domains.

III. Results

A. 2D simulation

The 2D simulation successfully replicates the results reported in [5] [Fig. 1B]. The square LV region has a lower resting membrane potential than the surrounding RV tissue [Fig. 1B]. Initiation of spiral wave activity results in the formation of a stable rotor that rotates at a steady rate within the LV region. The rotor is the source of wavefronts that smoothly propagates away from the rotor. Smooth propagation is disrupted when the wavefront encounters the LV/RV border. The longer APD of the RV tissue translates to a longer refractory period. As the wavefronts propagate towards the border, the RV tissue is still not recovered from the previous excitation. The propagating wave encounters unexcitable tissue and the continuity of the wavefront is disrupted. This leads to wave breakup which can lead to the formation of ephemeral spiral waves at the periphery of the LV tissue. These spiral waves do not last long enough to propagate into the LV. The mother rotor is left unperturbed throughout the simulation. This establishes the maintenance of the stable spiral wave in the LV that drives the fibrillatory activity in the tissue.

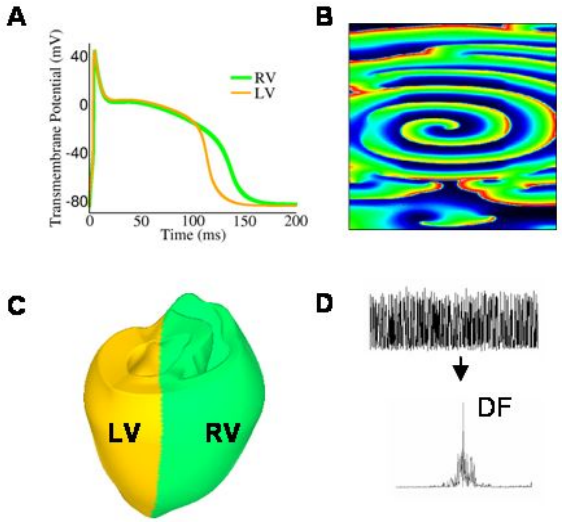

Fig. 1. A) Action potential of LV and RV with respective IK1 modification. B) 4 cm x 4 cm 2D sheet with a 2 cm x 2 cm square region in the middle that is modeled as LV tissue and the rest as RV tissue. C) 3D model of rabbit ventricle color coded to show LV and RV regions. D) Sample transmembrane potential trace during 7 seconds of VF and the corresponding FFT power spectrum. The peak is the dominant frequency for that node.

B. 3D simulation

The mechanism for wave breakup and rotor production observed in the 2D simulation is also observed in the 3D simulation. Fig. 2A presents an epicardial view of the boundary between LV and RV taken during the delivery of the 20 Hz pulse on the LV epicardium. At t=60 ms the wavefront from the first pulse propagates towards the RV. 100 ms later, the boundary between the two regions is clearly demarcated by the slowly recovering tissue on the RV side of the boundary. At t=210 ms, the wavefront from the third pulse encounters the refractory tail from the previous wavefront and breakup ensues. The proceeding pictures outline the formation of a rotor. When the delivery of the pulses is stopped, the rotor activity persists and generates further wave break-ups as the ventricle degenerates into a full case of VF.

Contrary to what is observed in the 2D experiment, the 3D simulation does not exhibit the formation of a single robust rotor in the LV. Although rotors that persisted for hundreds of ms are observed, none lasted the entire seven seconds of VF [Fig. 2B]. The formation of robust rotors is not limited to the LV. At various times, robust rotors form in the septum and the RV (t=2 s). As VF progresses, a regular pattern arises. At t=5 s and t=6 s, planar waves dominate the activity in the RV while multiple rotors are visible on the LV. During this period in the simulation, the RV is unable to support the formation of a rotor. The electrical activity in the RV is driven by the erratic electrical activity emanating from the LV. Towards the end of the simulation (t=7 s), this organization is disrupted and a rotor forms on the RV while planar waves dominate the LV.

The lack of a single stable rotor is attributable to the complexity of the 3D model. Whereas a spiral wave on a 2D sheet can only be annihilated by activity lateral to it, the 3D ventricle has complex wave activity into the depth of the tissue [Fig. 3]. On Fig. 3A, the figure on the left is a transmembrane potential map of the LV epicardium that exhibits the appearance of ectopic-like activity. The figure on

the right reveals a rotor anchored in the LV endocardium is the source of the breakthrough activity. Fig. 3B is an example of transmural reentry that forms within the tissue. This reentry is located within the LV wall near the base of the ventricle. The reentry persists for 600 ms before a wavefront emanating from the apex disrupts its rotation. The transmural wave drifts and eventually surfaces on the LV epicardium. These electrical activities that originate from within the myocardium appear intermittently throughout the simulation. Depending on the activity around them, they disrupt rotor activity or breakup and become a source of meandering wavelets. The map of the total number of phase singularities (PS) underlines the instability and prevalence of rotors [Fig. 3C]. Each PS corresponds to the presence of a core of reentry. The results show that the prevalence of core formation is not limited to a single region. Throughout the VF episode, rotors tend to form within the LV wall and the septum. The formation of drifting intramural waves within the LV and the septum leads to higher PS count than the RV. Despite the fact that the septum is modeled as part of the RV, the thick geometry of the septum allowed for the support of rotor formation.

The potential recordings of each myocardial node exhibit the rapid and irregular trace typical of VF [Fig. 1D]. The power spectrum obtained from FFT yields the presence of a dominant frequency (DF). Fig. 4 is the corresponding DF maps for the LV and RV epicardium and cross sectional slices of the ventricles. The DF in the LV region ranges from 27.6 Hz to 32.9 Hz with a mean±SD of 29.7±1.006 Hz. The RV has a range of 26.6 Hz to 33.4 Hz with a mean±SD of 29.5±0.912 Hz. This contrasts with Samie et al.'s findings where they found a significantly higher mean frequency in the LV as compared to the RV. They reported differences of up to 12 Hz between the two ventricles. This differs significantly from our results which exhibit a low range of DF.

The DF maps exhibit the presence of domains of similar

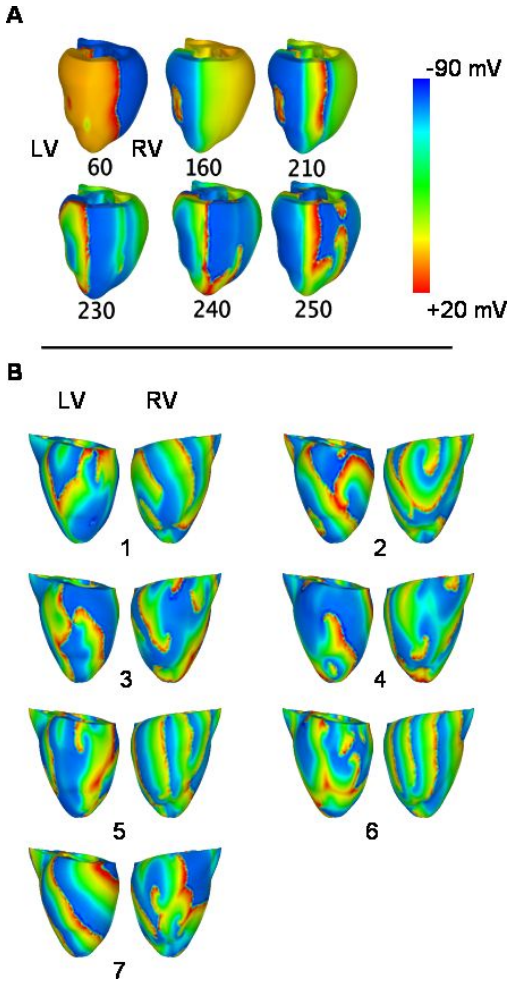

Fig. 2. A) Transmembrane potential map during the delivery of fast pacing on LV with a view of the border between the LV and the RV. The border is the site of the first wave breakup and subsequent production of a rotor. The number underneath each figure is the time in milliseconds. t=0 corresponds to the time when first fast pacing stimulus is delivered. B) Evolution of VF throughout the 7 seconds of simulation with corresponding views of the LV and RV epicardium. The number underneath each pair of figures is the time in seconds. t=0 corresponds to time when fast pacing is terminated.

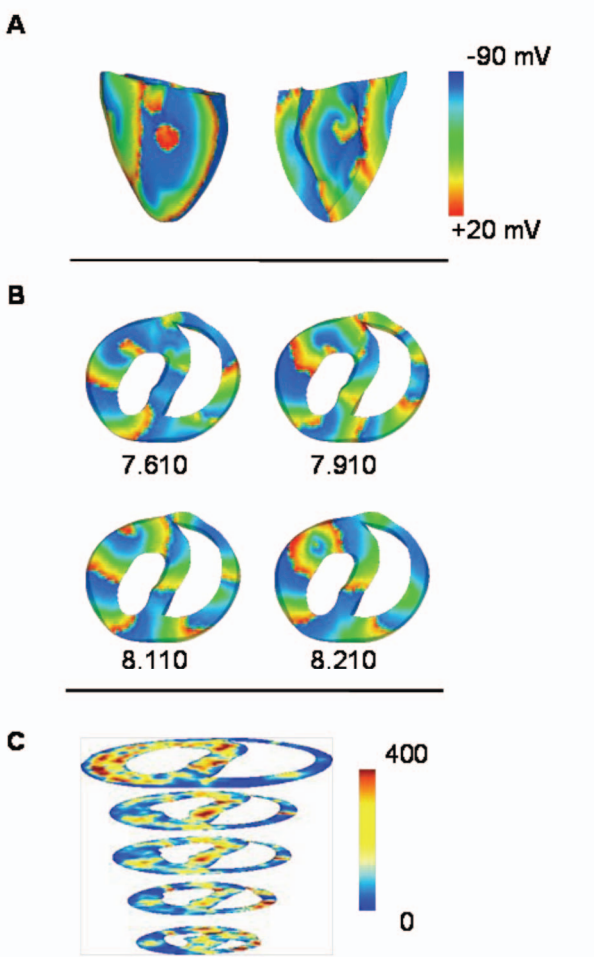

Fig. 3. A) The left picture is an epicardial view with breakthrough activity. The right picture is a view into the ventricle which shows that the source of the breakthrough is a rotor that is anchored in the endocardium. B) Cross sectional slice near the base of the ventricle shows the formation of a transmural reentry. The number at the bottom of each figure is the time in seconds. C) Total number of phase singularities (PS) in the ventricle. PS is the organizing center of rotors.

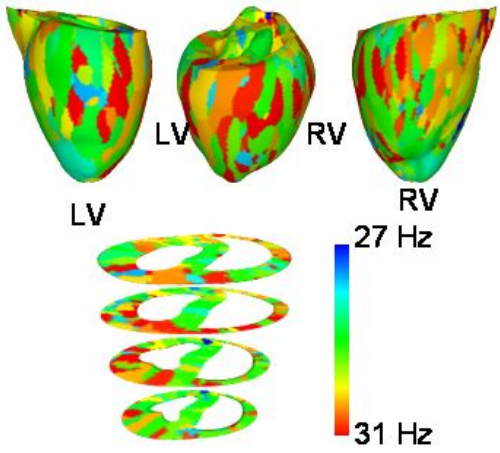

Fig. 4. Dominant frequency maps of the epicardial surface with views of the LV, LV and RV boundary, and the RV and cross-sectional slices of the ventricle showing the intramural dominant frequency

frequency. A sizeable high frequency domain is present at the border between the RV and LV region. Since no stable rotor was observed in this region, the slightly higher dominant frequency is attributable to increased activation due to wave breakups at this site. This supports the previous observation that the LV/RV border promotes the formation of fibrillatory activity via wave breakup due to differences in refractoriness.

IV. Discussion

Experimental studies of VF have been limited to views of cardiac electrical activity at the surface. Our sophisticated model of the rabbit ventricle addresses this limitability by providing an insight into the transmural events that occur during VF. Previous 2D experiments [5] that were replicated in this study show that differences in one ionic current can lead to different spiral wave dynamics. In particular, larger outward conductance of the IK1 current in the LV, which leads to a shortened APD, results in the formation of a stable, high frequency spiral wave. A single rotating source that drives wave break-up is observed when LV tissue is coupled with RV tissue.

Our study has shown that such spiral wave behavior does not translate to a 3D model. Although, the border between the LV and RV still play a role in the initiation and maintenance of VF via the formation of areas of different refractoriness, we do not observe the formation of a single rotor that drives the activity in the rest of the tissue.

The lack of a driving rotor is directly attributable to the 3D nature of ventricles. Multiple competing rotors can be present at the same time on the endocardium and epicardium. Within the thicker parts of the tissue, such as the LV wall and the septum, intramural reentry is also supported. These rotors drift and collide with each other causing the disruption of the formation of a stable rotor. Lack of methodology prevents experimentalists from visualizing transmural events. But modeling studies [9] confirm that incorporation of rotational fiber orientation in a 3D structure leads to the destabilization of scroll waves and results in wave breakup. The current study imparts insight into the inherent complexity brought about by a 3D space in the organization of rotor dynamics.

Although a single driving rotor is not seen in this study, this does not necessarily nullify the mother rotor hypothesis. Whereas this study only investigates the effect of incorporating one type of heterogeneity, there are multitudes more present in the heart. Studies have shown that anatomical heterogeneities, such as the papillary muscle insertions in the LV endocardium, can provide the anchor for a stable rotor [10][11].

References

[1] A. V. Zaitsev, O. Berenfeld, S. F. Mironov, J. Jalife, and A. M. Pertsov, "Distribution of excitation frequencies on the epicardial and endocardial surface of fibrillating ventricular wall of the sheep heart", *Circ Res*, vol. 86, pp. 408-417, 2000.

[2] A. Panfilov, and A. Pertsov, "Ventricular fibrillation: evolution of the multiple-wavelet hypothesis", *Phil Trans R Soc Lond*, vol. 359, pp. 1315-1325, 2001.

[3] B-R. Choi, W. Nho, T. Liu, and G. Salama, "Life span of ventricular fibrillation frequencies", *Circ. Res.*, vol. 91, pp. 339-345, 2002.

[4] T-J. Wu, S-F. Lin, A. Baher, Z. Qu, A. Garfinkel, J. N. Weiss, C-T. Ting, and P-S. Chen, "Mother rotors and the mechanisms of D600-induced type 2 ventricular fibrillation", *Circulation*, vol. 110, pp. 2110-2118, 2004.

[5] F. H. Samie, O. Berenfeld, J. Anumonwo, S. F. Mironov, S. Udassi, J. Beaumont, S. Taffet, A. M. Pertsov, and J. Jalife, "Rectification of the background potassium: a determinant of rotor dynamics in ventricular fibrillation", *Circ Res*, vol. 89, pp. 1216-1223, 2001.

[6] C. Luo, and Y. Rudy, "A model of the ventricular cardiac action potential, depolarization, repolarization, and their interaction", *Circ Res*, vol. 68, pp 1501-1526, 1991.

[7] N. A. Trayanova, J. C. Eason, and F. Aguel, "Computer simulations of cardiac defibrillation: a look inside the heart", *Comput Visual Sci*, vol. 4, pp. 259-270, 2002.

[8] J. M. Meunier, J. C. Eason, and N. A. Trayanova, "Termination of reentry by a long-lasting AC shock in a slice of canine heart: a computational study", *J Cardiovascular Electrophysiology*, vol. 13, pp. 1253-1261, 2002.

[9] W-J. Rappel, "Filament instability and rotational tissue anisotropy: A numerical study using detailed cardiac models", *Chaos*, vol. 11, no.4, pp. 71-80, 2001.

[10] J. Huang, G. P. Walcott, C. R. Killingsworth, S. B. Melnick, J. M. Rogers, and R. E. Ideker, "Quantification of activation patterns during ventricular fibrillation in open-chest porcine left ventricle and septum", *Heart Rhythm*, vol. 5, pp. 720-728, 2005.

[11] J. M. Rogers, J. Huang, S. B. Melnick, and R. E. Ideker, "Sustained reentry in the left ventricle of fibrillating pig hearts", *Circ. Res.*, vol. 92, pp. 539-545, 20